

Characterization of open and suburban boundary layer wind turbulence in 2008 Hurricane Ike

S. Jung^{*1} and F.J. Masters²

¹Department of Civil and Environmental Engineering, Florida A&M University –
Florida State University College of Engineering, Tallahassee, FL 32310, USA

²Department of Civil and Coastal Engineering, University of Florida, Gainesville, FL 32611, USA

(Received March 28, 2012, Revised September 14, 2012, Accepted October 3, 2012)

Abstract. The majority of experiments to characterize the turbulence in the surface layer have been performed in flat, open expanses. In order to characterize the turbulence in built-up terrain, two mobile towers were deployed during Hurricane Ike (2008) in close proximity, but downwind of different terrain conditions: suburban and open. Due to the significant non-stationarity of the data primarily caused by changes in wind direction, empirical mode decomposition was employed to de-trend the signal. Analysis of the data showed that the along-wind mean turbulence intensity of the suburban terrain was 37% higher than that of the open terrain. For the mean vertical turbulence intensity, the increase for the suburban terrain was as high as 74%, which may have important implications in structural engineering. The gust factor of the suburban terrain was also 16% higher than that of the open terrain. Compared to non-hurricane spectral models, the obtained spectra showed significantly higher energy in low frequencies especially for the open terrain.

Keywords: hurricane; suburban; turbulence intensities; gust factors; integral scales; power spectra

1. Introduction

Since the 1950s, mechanical turbulence properties in the surface layer have been extensively characterized through research on non-tropical cyclone wind events (e.g., Lettau and Davidson 1957, Izumi 1971, Wieringa 1973, Izumi and Caughey 1976, Taylor and Teunissen 1987, Baas *et al.* 2009, Li *et al.* 2009). The few surface wind studies conducted in tropical cyclones (TC) have almost exclusively been performed in flat, open expanses such as airports and the countryside (e.g., Krayner and Marshall 1992, Masters *et al.* 2010, Schroeder and Smith 2003). Thus a relatively unexplored area is the turbulent nature of hurricane boundary layer winds occurring in built-up terrain. The need for research on this topic is due to the extensive property damage and loss caused by TCs worldwide, which largely occurs in population centers that by their nature are predominantly suburban.

The key contribution of this paper is a direct comparison of high fidelity wind velocity data collected from two instrumented towers that were co-located 2.2 km apart but in differing terrain conditions. The upwind terrain of the first location is built-up in all directions. The upwind terrain

*Corresponding author, Assistant Professor, E-mail: sjung@eng.fsu.edu

of the second observation site may be described as nominally flat and open to the east and suburban to the west. The towers simultaneously collected data throughout the passage of Hurricane Ike, including a full eyewall passage. The data exhibited non-stationarity trending due to the associated changes in wind speed and to a lesser extent, wind direction. This paper will address the nonstationary nature of the data and the empirical mode decomposition that was employed to remove the trend. The remainder of the paper will present detailed analysis of the gust factors, turbulence intensities, integral length scales, and the power spectra in the context of terrain dependence.

2. Hurricane Ike (2008) experimental details

Hurricane Ike made landfall on September 13, 2008 in Galveston, TX as a Category 2 hurricane on the Saffir-Simpson Hurricane Scale (Brown *et al.* 2010). Field research activities were coordinated through the Florida Coastal Monitoring Program (FCMP, fcmp.ce.ufl.edu) in the Houston, TX area and surroundings. Its infrastructure includes six 10-m mobile weather stations (Fig. 1) designed to withstand gust loading and debris generated by a strong Category 5 hurricane. The data acquisition system measures 3D wind speed and direction at 5- and 10-m and collects temperature, rainfall, barometric pressure, and relative humidity data at the tower's base. Data are sampled at 10 Hz using a National Instruments Labview system. Balderrama *et al.* (2011) provides a detailed description of the program.

Two RM Young anemometer systems—a custom array of three gill propellers (Model Number 27106R) and a wind monitor (Model Number 05103V)—collect data at the 10 m level, and a second array of gill propellers collects wind speed data at the 5 m level to measure winds at the approximate mean roof height of a single-story home. The gill anemometry is used in this study.



(a) T2 with tower stowed and outriggers deployed



(b) T3 fully deployed

Fig. 1 FCMP Weather Stations deployed in Baytown, TX

Dynamic characteristics of the anemometer's four-blade polypropylene helicoid propellers (Model Number 08234) include a 2.7 m 63% recovery distance constant and a damped natural wavelength of 7.4 m. The wind monitor is rated for a 100 m/s gust survival and has a 50% recovery vane delay distance of 1.3 m. The limitations caused by its frequency response characteristics are detailed in Schroeder and Smith (2003).

During Hurricane Ike, the FCMP erected four instrumented towers in Houston area and its surroundings. This paper compares the results of data collected from two towers (designated T2 and T3), which were deployed 2.2 km apart in Baytown, TX. The GPS coordinates of T2 are 29.811969 N, 94.901578 W, and that of T3 are 29.801944 N, 94.882221 W. The deployment sites were selected to compare the effect of the upwind exposure on hurricane wind turbulence. Fig. 2 shows the satellite view of the two towers.

The upwind exposure of T2 is primarily suburban. The weather station was located to the west of a neighboring subdivision, which contained 882 one- and two-story single-family dwellings in its 1000 m x 800 m tract. The nearest home was approximately 100 m, or approximately 10 obstacle heights, to the east. T3 is primarily open to the east and suburban elsewhere. The topography for the entire region was flat. Directionally dependent terrain characteristics are summarized in Table 1. To distinguish different combinations of upwind exposures, descriptions are provided for three timeframes designated Intervals A, B, and C. All wind directions are measured clockwise from the north.

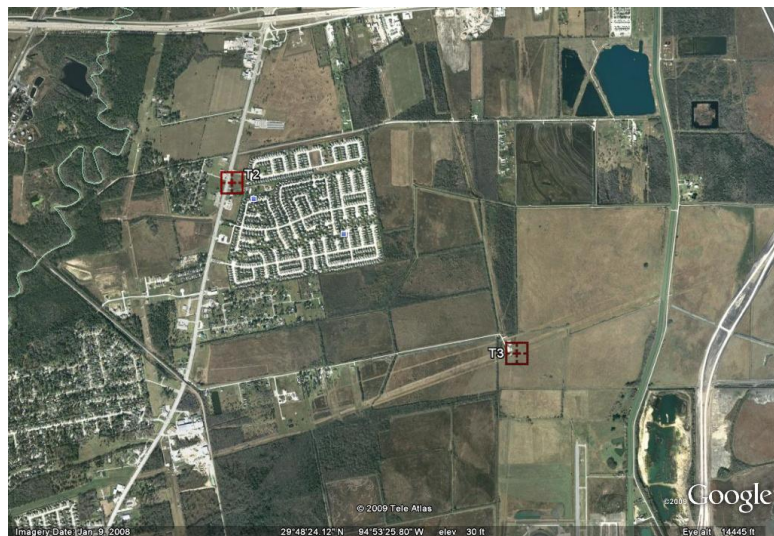


Fig. 2 Satellite view of the site near Eldon, Texas (Source: 29°48'24.12"N and 94°53'25.80"W, Google Earth)

3. Basic wind characteristics

Fig. 3 contains the mean wind direction, mean wind speed and the peak 3 s gust for 10-minute data segments collected by T2 and T3. The wind direction shifted continuously between 05Z-11Z (Interval B) and was nearly constant between 00Z-05Z (Interval A) and 11Z-18Z (Interval C). As

summarized in Table 1, the upwind terrain characteristics of T2 and T3 were distinctively different for Interval B, but they were marginally different or similar for the Intervals A and C.

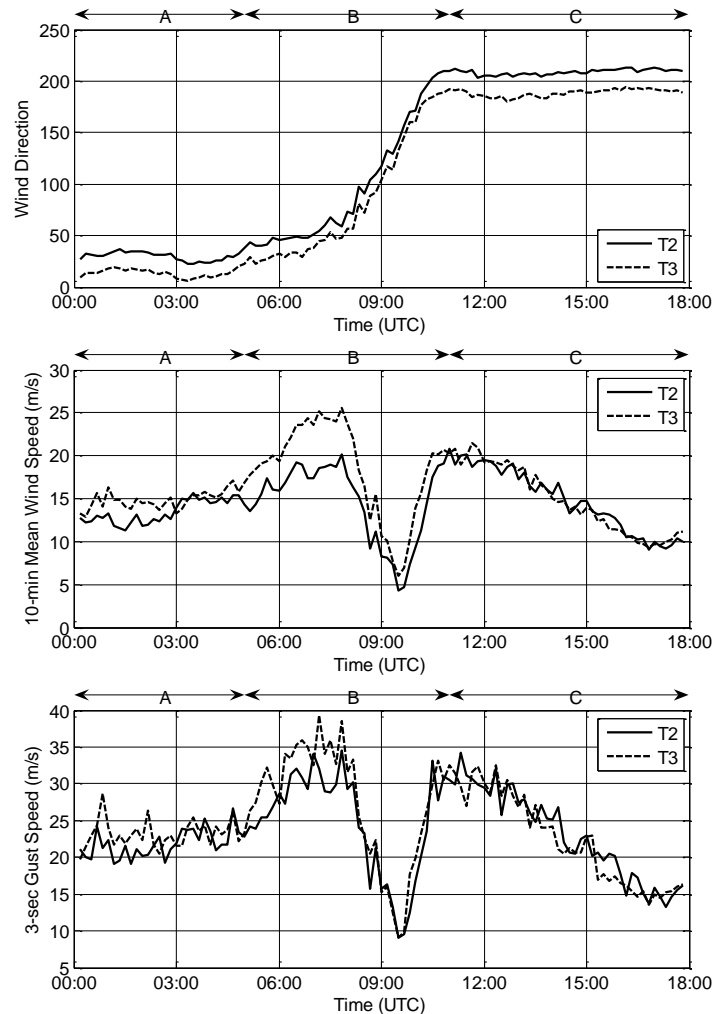


Fig. 3 The wind direction, speed, and 3-second gust calculated from 10-minute segments

During Interval A, the upwind terrain of T3 was relatively unobstructed compared to that of T2. The 10-minute mean wind speed was approximately 15 m/s and the gust speed was approximately 20-30 m/s. The wind speed and the gust of T3 were consistently higher than those of T2 as the upwind terrain was less built-up, but not significantly higher. The largest difference in wind speeds occurred during Interval B. At T3, the 10-minute wind speed ranged from 5-25 m/s, and the peak gust speed in each 10-min segment ranged from 10-40 m/s. The wind speed recorded at T3 was distinctively larger than that of T2 in the first half of Interval B, when the wind speed stayed high in the range of 15-25 m/s and the upwind terrain characteristics were completely different. In the

second half of Interval B (which corresponds to the eyewall passage), the difference in the wind speed was not as significant because the upwind terrain characteristics became similar to each other. During Interval C, there was almost no difference of the wind speed between T2 and T3 because the upwind terrain characteristics were similar to each other.

The comparison of peak gust values is of particular interest. Most building codes and standards use an open exposure gust speed at 10 m to calculate the freestream velocity pressure, which in turn, is used to compute the pressures that act on the building surfaces. T2 recorded a peak 3 s moving average gust speeds of 21.9 m/s, 24.7 m/s and 23.1 m/s for the intervals A, B and C, respectively. The corresponding values for T3 were 23.2 m/s, 27.3 m/s and 22.5 m/s for the intervals A, B and C. The corresponding T2:T3 ratios were 0.94, 0.90, and 1.03. The ratio for Interval B, which contains the peak gust values from suburban and open exposure, is found to be consistent with the gust ratio contained in ASCE 7-10 (2010). The ASCE 7 gust ratio may be computed from the square root of the velocity pressure exposure coefficient (K_z), which is the conversion factor that is multiplied by the gust velocity pressure at 10 m in flat, open country terrain to give the corresponding gust velocity pressure for a specified terrain and height. The corresponding multiplier to convert velocity can be computed from the square root of this value since the pressure is proportional the velocity squared. At a 10 m height in suburban terrain, $K_z = 0.72$ for 10 m. The measured value of 0.90 is within five percent of $\sqrt{0.72} = 0.86$, which gives reasonable agreement.

Table 1 Description of the upwind terrain at the tower sites

Interval ID	Time (UTC)	T2		T3	
		Direction	Description of terrain	Direction	Description of terrain
A	0:00 ~ 5:00	(23°, 41°)	Some low-rise buildings and I-10 between 0~2 km upwind	(6°, 26°)	Open terrain between 0~1km upwind; some vegetation between 1~2 km upwind
B	5:00 ~ 11:00	(44°, 211°)	Suburban structures between 0~1km upwind; some vegetation between 1~2 km upwind	(29°, 191°)	Open terrain between 0~1km upwind; mixture of open terrain and some vegetation between 1~2 km upwind
C	11:00 ~ 18:00	(205°, 212°)	Combination of suburban structures and some vegetation between 0~2 km upwind	(182°, 193°)	Combination of open terrain with some vegetation between 0~2 km upwind

4. Non-stationary nature of the hurricane wind data

Over a long enough interval, wind velocity time series recorded during a TC passage are inherently non-stationary. The structure of the storm itself is such that the maximum wind speed typically occurs 10-50 km outward from the center of circulation at or near the eyewall. The winds decay inwardly (in the eyewall) and outwardly for hundreds of kilometers until ambient conditions

occur. Thus a storm translating over a fixed observation point results in non-stationary trend. This is evident in Fig. 3, which shows the entire passage as recorded by T2 and T3.

Table 2 Summary of the run test for 1-hour time-series of the longitudinal wind speed at 10 m

Interval ID	Beginning time of the 1-hour time-series (UTC)	T2		T3	
		Passed the run test	Passing percentage	Passed the run test	Passing percentage
A	0:00	*	100	*	100
	1:00	*			
	2:00	*			
	3:00	*			
	4:00	*			
B	5:00	*	34	*	17
	6:00				
	7:00	*			
	8:00				
	10:00				
C	11:00	*	71	*	71
	12:00	*			
	13:00	*			
	14:00				
	15:00	*			
	16:00				
	17:00	*			
		Total %	67	Total %	61

Stationarity tests were performed on the data using the run test (Bendat and Piersol 1986) to quantify the non-stationarity systematically. One-hour time-series of the longitudinal wind speed were divided into 30 equal time intervals, and then mean square values for all intervals were computed. The mean square values were used as an input to the run test with a level of significance of 0.05. If the signals passed the run test, it indicates that there is no evidence of an underlying trend, or that the time-series can be considered stationary. The run tests were performed for all 36 one-hour time-series from T2 and T3. The results are summarized in Table 2. It was explained in the previous section that the data from 00Z-05Z (Interval B) provided the best opportunity to study the effect of the upwind exposure, because the wind directly passed through the suburban area before reaching T2 whereas T3 maintained open terrain characteristics. However, Table 2 shows that the data from Interval B is highly non-stationary compared to other data. Only 34% of T2 data and 17% of T3 data passed the run test. Thus de-trending was implemented, which is the subject of the next section. Table 2 used one-hour time-series in order to quantify and explain the division of Intervals A, B, and C. However, hurricane winds typically show rapid change of speed and direction for much shorter time-series. Further analyses starting the next section will be based on 10-minute segments in order to account for this rapid change.

5. De-trending using empirical mode decomposition (EMD)

Different meteorological phenomena show different characteristics of non-stationarity, and therefore the scientific community in general does not have a consensus on the best method for de-trending (Andreas *et al.* 2008). In this analysis, the empirical mode decomposition (EMD) was employed because it has performed robustly compared to other methods (Huang *et al.* 1998). The EMD has been successfully applied to non-stationary wind speed records, including hurricane events (Xu and Chen 2004, Chen and Xu 2004, Chen *et al.* 2007).

The EMD was developed for analyzing nonlinear and non-stationary time series (Huang *et al.* 1998). It identifies the intrinsic oscillatory characteristics of the data, and decomposes them into intrinsic mode functions (IMFs). For the time-series $x(t)$, the decomposition is described as

$$x(t) = \sum_{i=1}^n c_i + r_n \quad (1)$$

in which c_i is the i^{th} intrinsic mode function and r_n is the residue. To obtain an IMF, the EMD creates envelopes using local minima and maxima, and then repeats a process called sifting to eliminate riding waves and to smooth uneven amplitudes. Further details of the EMD can be found from (Huang *et al.* 1998, Huang 2005).

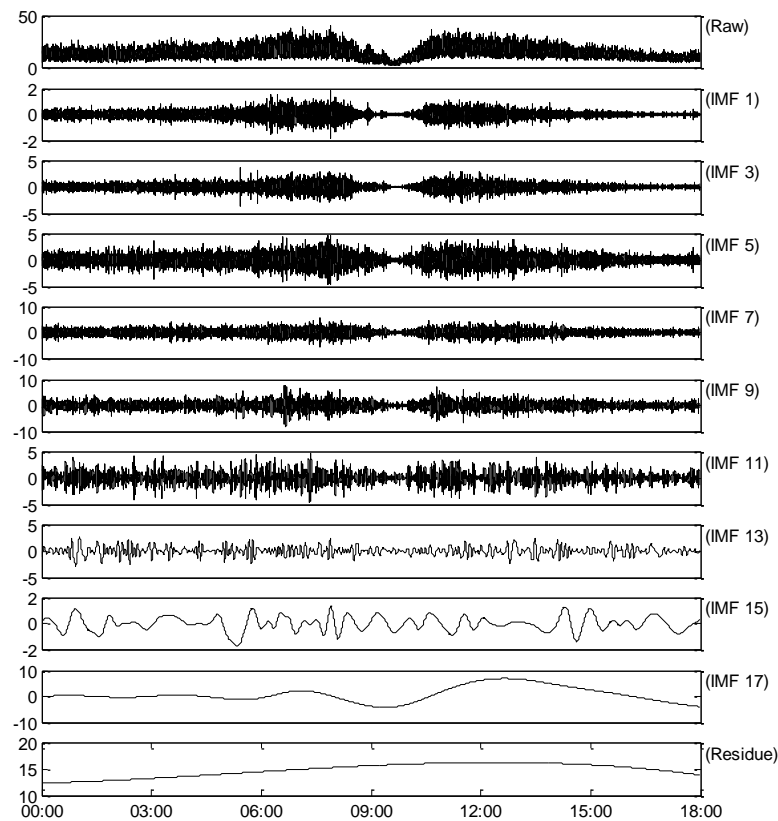


Fig. 4 Example empirical mode decomposition (EMD) of the raw wind data from T2, longitudinal component

In order to demonstrate how the EMD is used for de-trending, it is applied to the longitudinal wind speed from T2. The top plot in Fig. 4 contains the raw wind speed data. The rest of the plots in Fig. 4 show the selected IMFs and the residue identified by the EMD. For some applications, the residue r_n in Eq. (1) is equal to the trend in the time-series. Previous studies (Xu and Chen 2004, Chen and Xu 2004) have found that higher intrinsic mode functions with very low frequency content contribute to the trending in hurricane surface winds. According to their application of the EMD to typhoon winds, the “final residue cannot represent the trend of wind speed, and the sum of the last a few IMF components plus the final residue may be used to describe its trend” (Chen and Xu 2004). Our investigations led to the same conclusion. In the examples of this paper, 0.01 Hz filter was used to obtain the IMFs to describe the trend.

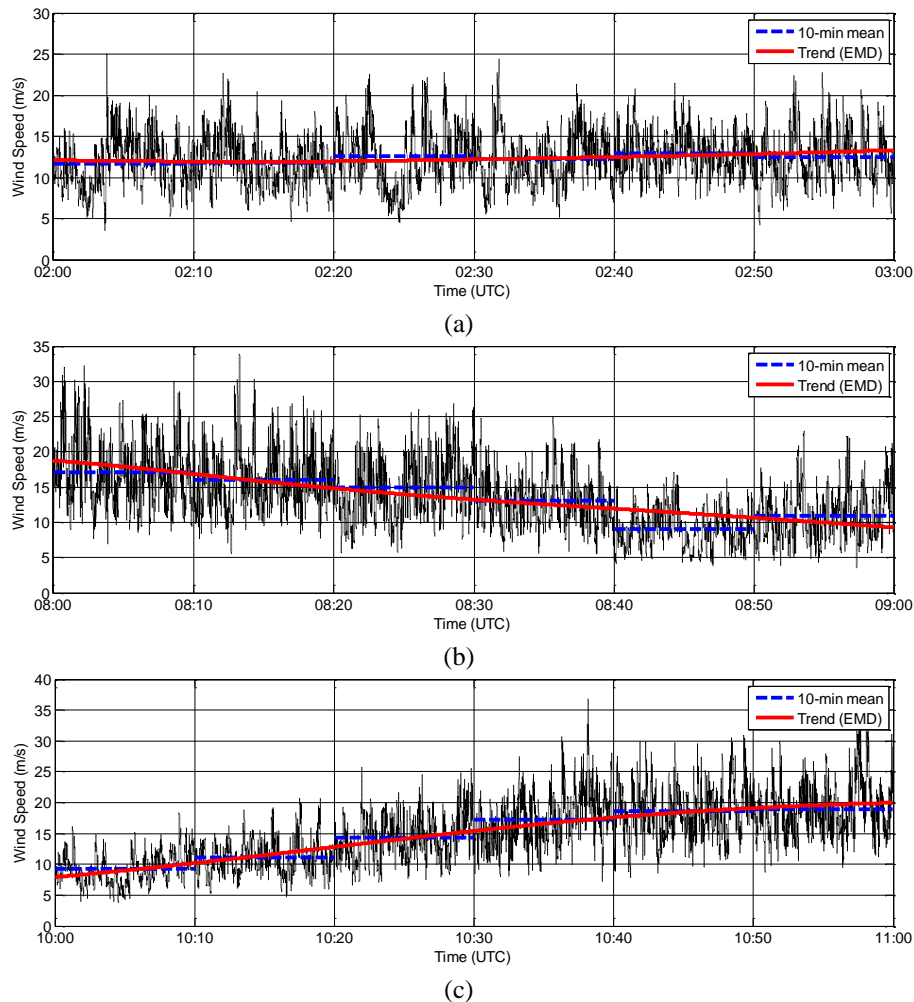


Fig. 5 Comparison of measured wind speed, 10-min mean speed, and the trend obtained from EMD for selected segments (All from T2; (a) UTC 2:00~3:00, (b) UTC 8:00~9:00 and (c) UTC 10:00~11:00)

Fig. 5 illustrates the performance of the EMD in obtaining the trend. Since all analyses in the paper are based on 10-min segments, 10-min means are also plotted for comparison. Fig. 5 (a) corresponds to the wind speed of T2 between 02Z-03Z. The data is stationary, and the trend obtained by the EMD is almost the same as the mean speed. Other stationary or near stationary time-series not presented herein also showed similar robustness of the EMD. When the EMD was applied to stationary or near stationary time-series, it obtained the trend very similar to the mean value. Therefore, we were able to apply the EMD consistently to all time-series without negatively affecting the analysis. The wind speed records shown in Figs. 5(b) and 5(c) are non-stationary.

They show qualitatively that the EMD identifies the trend successfully. The trend was obtained using the entire time series. Compared to the discrete 10-min means, the trend identified by EMD is much more natural without arbitrary jumps between 10 minute intervals.

Table 3 Normality test of the de-trended 10-min segments, for longitudinal wind speed at 10 m

Interval ID	Percentage passing the normality test			
	T2		T3	
	EMD	Linear	EMD	Linear
A	94	95	95	96
B	88	88	94	94
C	93	93	95	94

Assuming that fluctuations in the longitudinal turbulence are adequately described by a Gaussian distribution, then a test for normality is a good indicator of the effectiveness of a de-trending technique. After de-trending the entire time series, they were segmented into 10-min non-overlapping blocks to check the normality. The Lilliefors normality test (Lilliefors 1967) was applied to each segment to determine if the de-trended data follow a Gaussian distribution. The test was performed with a 1% level of significance. The test for each 10-min block was repeated 100 times, with 100 randomly drawn samples each time. Table 3 contains the percentage of records passing the normality test for EMD and linear de-trending. Both methods perform similarly in terms of passing the normality test. However, as shown in Figs. 5(b) and 5(c), EMD de-trending offers much more natural representation of the trend without the discontinuity.

The major shortcoming of applying the EMD to surface layer winds is that it does not filter the variance proportionally to the change in the mean wind speed. Essentially it behaves like a low-pass filter. However, the nature of the boundary layer turbulence is that the standard deviation of the fluctuating wind component is expected to increase linearly with wind speed (owing to the energy cascade). Applying an EMD to de-trend the data removes the first order non-stationarity, but the higher order non-stationarity remains. The practical implication is that large changes within the time-varying mean wind speed result in large changes in the signal variance. For example, see Fig. 5(c). The amplitude of the fluctuating component of the wind speed is proportional to the time-varying mean wind speed. To address this issue, the duration of the record segments must be chosen to limit the effects of the changing variance. We have found that a 10 min is a reasonable

duration, by comparing the standard deviation computed from the first half and the second half of the segment. In case of the along wind speed at 10 m, the average difference in standard deviation was 12.1% for T2 and 11.9% for T3.

An alternative approach of addressing the non-stationarity is to use shorter duration segments. For examples, some studies reported that 5-min segments of hurricane wind data were nearly stationary (Schroeder and Smith 2003, Caracoglia and Jones 2009). However, in such an approach, the length of the segment may have to change depending on the characteristics of the hurricane (Schroeder and Smith 2003). The merit of the EMD de-trending is that it can be applied to any segment length of choice.

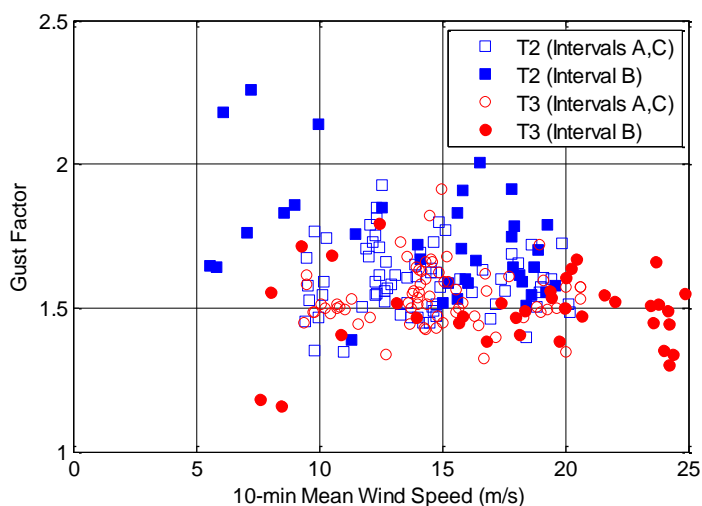


Fig. 6 Distribution of gust factors for various mean wind speeds (3-sec peak speed and 10-min mean wind speed)

6. Comparison of gust factors

A gust factor (GF) is the ratio of the peak wind speed inside a record to the mean wind speed of that record. To account for the non-stationarity, the trend identified using EMD is used to calculate the mean wind speed. Gust factors are calculated for 10-min segments from both weather stations.

Fig. 6 shows the distribution of GF ($T = 60$ s, $t = 3$ s) versus mean wind speed. Hollow symbols designate values from Intervals A and C whereas solid symbols indicate values from Interval B. The GFs T2 and T3 have a similar spread during Intervals A and C. However, the GFs of T2 are clearly larger than those of T3 in Interval B. Table 4 contains the mean GFs of the three intervals. The mean GFs for T3 for Intervals A, B, and C are 1.57, 1.49, and 1.52 respectively. The corresponding mean GFs for T2 are 1.65, 1.73 and 1.56, which are 5%, 16% and 3% larger than their T3 counterparts.

Interval B results are now discussed. The GF measured by T3 (1.49) is considered to be a representative open country value. It compares favorably with the theoretical open exposure value (~ 1.46) determined from a crossing rate approach described in Masters *et al.* (2010), which utilizes

the von Karman spectrum and a modified form of the Harris and Deaves (1981) longitudinal turbulence intensity model. Using the same approach with the original Harris and Deaves (1981) model would yield a GF ($T = 60$ s, $t = 3$ s) = 1.53. Comparison to data collected at coastal airports during tropical cyclones is also favorable. Vickery and Skerlj (2005) computed an open exposure hourly mean gust factor of 1.55 using the data from 12 different hurricanes. The GF measured by T2 (1.74) is considered to be a representative suburban value. Its corresponding theoretical z_0 value is 0.32 m using the ESDU (2010) approach found in Vickery and Skerlj (2005), which is very close the mean z_0 value of 0.30 m defined for Exposure B in ASCE 7-10. It is also noted that this definition only applies where the surface roughness B condition exists 800 m upwind. Suburban conditions spanned 800-900 m during the study interval.

Table 4 Mean gust factors for T2 and T3 (3-sec peak seed and 10-min mean speed)

Interval ID	Gust factor	
	T2	T3
A	1.65	1.57
B	1.73	1.49
C	1.56	1.52

7. Comparison of turbulence intensities

The turbulence intensity is simple yet important descriptor of atmospheric turbulence. For the longitudinal wind (along-wind) component, the fluctuating component of the stationary wind is defined as

$$u(t) = U(t) - \bar{U} \tag{2}$$

in which $U(t)$ is the instantaneous speed and \bar{U} is the mean speed for a predefined time period. The longitudinal turbulence intensity is defined as

$$I_u = \frac{\overline{u^2}^{1/2}}{\bar{U}} \tag{3}$$

in which $\overline{u^2}^{1/2}$ is the root mean square of the fluctuating component. The turbulence intensities for the lateral (across-wind) and vertical directions are defined similarly, but referenced to the longitudinal mean.

As illustrated in Figs. 5(b) and 5(c), the wind speed data is strongly non-stationary during the approach and passage of the eyewall. To address the non-stationarity, the trend identified using the EMD is used to obtain the fluctuating component. Therefore, the fluctuating component and the turbulence intensity for the non-stationary wind are calculated as

$$u(t) = U(t) - \overline{U'}(t) \quad (4)$$

$$I_u = \frac{\overline{u^2}^{1/2}}{\overline{U'}} \quad (5)$$

in which $\overline{U'}(t)$ is the trend identified using the EMD and $\overline{U'}$ is the mean value of $\overline{U'}(t)$ for a predefined time period. Since the turbulence intensity depends on the predefined time period, too short averaging time should not be used. Schroeder and Smith (2003) reported that the variation of the turbulence intensity levels off when the averaging time is between 5 and 10 minutes. An averaging time of 10 minutes is used in this paper. Note that $\overline{U'}$ was used only when the turbulence intensity was computed using the EMD trend. Conventional \overline{U} was used when the mean wind speed was computed for other cases.

Fig. 7 shows time history of 10-min longitudinal turbulence intensities of T2 and T3 and their ratio. For concise description, they will be referred to as I_u^{T2} , I_u^{T3} , and I_u^{T2}/I_u^{T3} . Tables 5 and 6 summarize the statistics of the data shown in the figure. The difference in terrain characteristics of Intervals A, B, and C is directly reflected in the turbulence intensities. In Interval A, terrain of T2 is slightly rougher than T3. The mean values of I_u^{T2} are 0.244 and 0.253, and mean values of I_u^{T3} are 0.215 and 0.234 for 10 m and 5 m, respectively. The mean values of I_u^{T2}/I_u^{T3} are 1.15 and 1.10 for 10 m and 5 m, respectively. Other statistical measures also indicate a marginal increase of the turbulence intensity for T2. In Interval C, the terrain characteristics of T2 and T3 are similar, and the statistics of the turbulence intensities show smaller difference than the Interval A.

The most important comparison of turbulence intensities is obtained from Interval B. T2 has suburban structures between 0~1 km upwind and some vegetation between 1~2 km. On the other hand, T3 has completely open terrain between 0~1 km and combination of open terrain and some vegetation between 1~2 km upwind. Consequently, the longitudinal turbulence intensities show clear difference between the two towers. The mean values of I_u^{T2} are 0.265 and 0.259, and mean values of I_u^{T3} are 0.196 and 0.205 for 10 m and 5 m, respectively. The mean value of I_u^{T2}/I_u^{T3} at 10 m is 1.37, or approximately a 40% increase in the turbulence intensity for the suburban terrain compared to the open terrain. At 5 m, the mean value of I_u^{T2}/I_u^{T3} is 1.27, or approximately a 30% increase. Unlike Intervals A and C, the minimum I_u^{T2}/I_u^{T3} at both 10 m and 5 m are about 1.0 meaning that I_u^{T2} is at least as large as I_u^{T3} . The maximum I_u^{T2}/I_u^{T3} is 1.92 for 10 m and 1.58 for 5 m. The turbulence intensities in Fig. 7 do not show the artificial peak observed by Schroeder and Smith (2003), which we believe is due to the EMD process employed in this paper. Therefore, it would be reasonable to conclude that the 10-min turbulence intensity of the suburban terrain may become two times higher than that of the open terrain at 10 m. At 5 m, the turbulence intensity of the suburban terrain may become 60% larger than that of the open terrain. Both the mean and the maximum values indicate that the effect of the terrain on the turbulence is more pronounced at 10 m than 5 m.

Another interesting observation is the effect of the wind speed on the turbulence intensity. The turbulence intensity of T2 moderately increases when the wind speed reduces between 08Z-10Z, which is consistent with the previous research (Ishizaki 1983). However, for open terrain, the

turbulence intensity does not change as much due to the change in the wind speed, which is consistent with observations made by Schroeder and Smith (2003). The turbulence intensity of T3 between 08Z-10Z clearly shows the difference compared to that of T2. In their research, the turbulence intensity of the airport (open) terrain is virtually unaffected by the change in the wind speed, whereas that of the transitional (rough) terrain increases due to the decrease in the mean wind speed. Fig. 8 plots turbulence intensities for various mean wind speeds for easier comparison. As explained above, T2 shows more rapid change in the turbulence intensity due to the change in the wind speed.

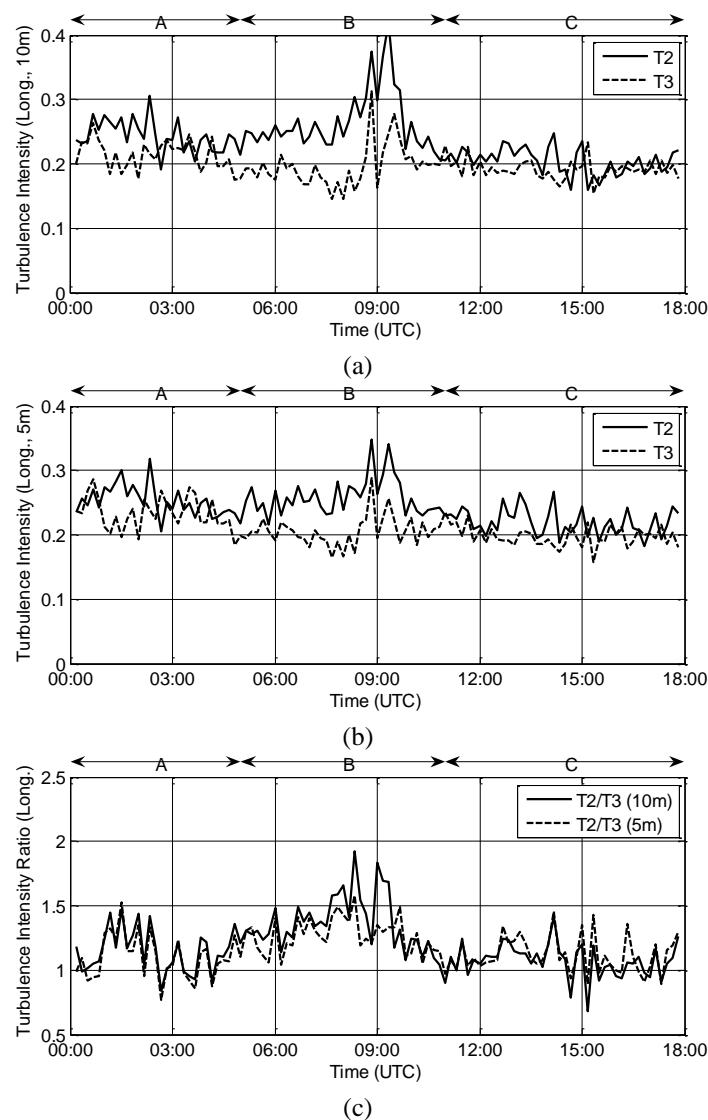


Fig. 7 Time history of (a) longitudinal turbulence intensities (10 m), (b) longitudinal turbulence intensities (5 m) and (c) their ratio between T2 and T3

Table 5 Statistics of the turbulence intensities of T2 and T3, and the statistics of the ratio (T2/T3) of the turbulence intensities (10 m)

Interval ID	Statistical measure	Longitudinal			Lateral			Vertical		
		T2	T3	T2/T3	T2	T3	T2/T3	T2	T3	T2/T3
A	Mean	0.244	0.215	1.15	0.145	0.111	1.32	0.090	0.073	1.24
	Standard deviation	0.025	0.022	0.17	0.011	0.010	0.14	0.004	0.006	0.10
	Maximum	0.306	0.263	1.47	0.171	0.139	1.68	0.099	0.081	1.43
	Minimum	0.191	0.175	0.84	0.125	0.088	1.06	0.082	0.060	1.10
B	Mean	0.265	0.196	1.37	0.175	0.124	1.43	0.114	0.067	1.74
	Standard deviation	0.047	0.033	0.21	0.023	0.018	0.18	0.024	0.008	0.36
	Maximum	0.417	0.312	1.92	0.225	0.171	1.84	0.166	0.094	2.34
	Minimum	0.207	0.146	1.04	0.123	0.076	1.05	0.062	0.053	0.80
C	Mean	0.204	0.192	1.07	0.139	0.124	1.13	0.068	0.087	0.79
	Standard deviation	0.020	0.015	0.13	0.012	0.013	0.15	0.005	0.009	0.12
	Maximum	0.247	0.234	1.41	0.169	0.162	1.47	0.080	0.107	1.07
	Minimum	0.159	0.154	0.68	0.112	0.105	0.81	0.054	0.075	0.59

Table 6 Statistics of the turbulence intensities of T2 and T3, and the statistics of the ratio (T2/T3) of the turbulence intensities (5 m)

Interval ID	Statistical measure	Longitudinal			Lateral			Vertical		
		T2	T3	T2/T3	T2	T3	T2/T3	T2	T3	T2/T3
A	Mean	0.253	0.234	1.10	0.137	0.132	1.06	0.082	0.074	1.13
	Standard deviation	0.023	0.025	0.18	0.015	0.021	0.17	0.007	0.009	0.18
	Maximum	0.318	0.286	1.53	0.167	0.183	1.49	0.095	0.091	1.48
	Minimum	0.206	0.184	0.77	0.114	0.098	0.71	0.072	0.056	0.82
B	Mean	0.259	0.205	1.27	0.165	0.124	1.34	0.109	0.068	1.59
	Standard deviation	0.029	0.023	0.14	0.038	0.019	0.30	0.025	0.009	0.24
	Maximum	0.348	0.287	1.58	0.254	0.174	2.10	0.182	0.099	1.95
	Minimum	0.216	0.165	1.04	0.104	0.090	0.81	0.066	0.056	0.99
C	Mean	0.220	0.198	1.12	0.113	0.132	0.86	0.074	0.067	1.12
	Standard deviation	0.021	0.016	0.14	0.015	0.014	0.15	0.005	0.004	0.10
	Maximum	0.267	0.236	1.46	0.143	0.171	1.16	0.085	0.079	1.35
	Minimum	0.183	0.158	0.89	0.080	0.104	0.58	0.063	0.059	0.89

The results of analyses of the lateral and vertical turbulence intensities are summarized in Figs. 9, 10 and Tables 5 and 6. Both the lateral and vertical turbulence intensities increase for the suburban terrain (T2) compared to the open terrain (T3) in Interval B. The increase is more significant for the vertical turbulence intensity whereas less so for the lateral turbulence intensity. Finally, the ratio between the lateral and the longitudinal turbulence intensities, and the vertical and the longitudinal turbulence intensities for both towers are plotted in Fig. 11. No significant difference is observed between T2 and T3.

Comparison of Figs. 7(c), 9(c) and 10(c) indicates that the terrain affects the vertical turbulence more than the longitudinal or lateral turbulence, which may have important implications in structural engineering. As shown in Tables 5 and 6, the mean values of I_w^{T2} / I_w^{T3} at 10 m and 5 m are 1.74 and 1.59, which are higher than those of I_u^{T2} / I_u^{T3} by 27% and 25%. The maximum values of I_w^{T2} / I_w^{T3} at both heights, 2.34 and 1.95, are also higher than those of I_u^{T2} / I_u^{T3} by 22% and 23%.

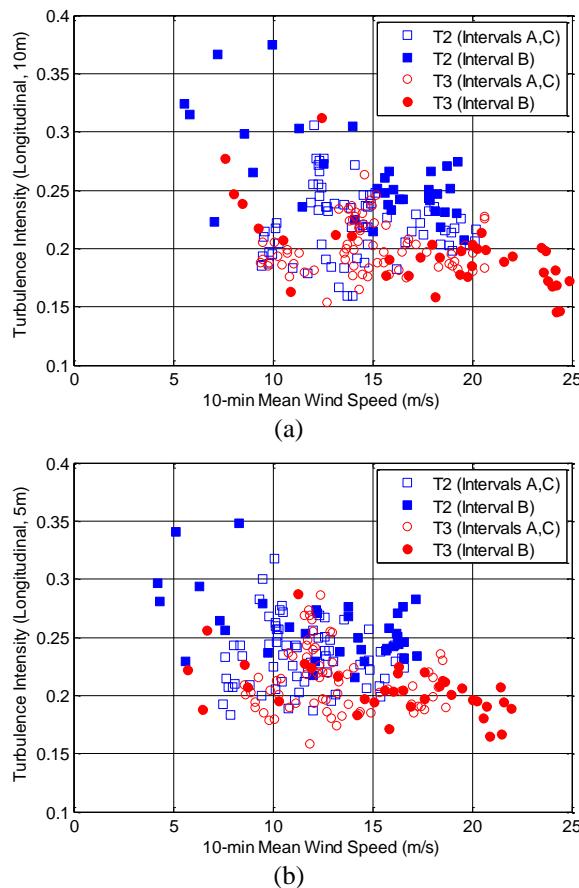


Fig. 8 Distribution of turbulence intensities (longitudinal) for various mean wind speeds ((a) 10 m and (b) 5 m)

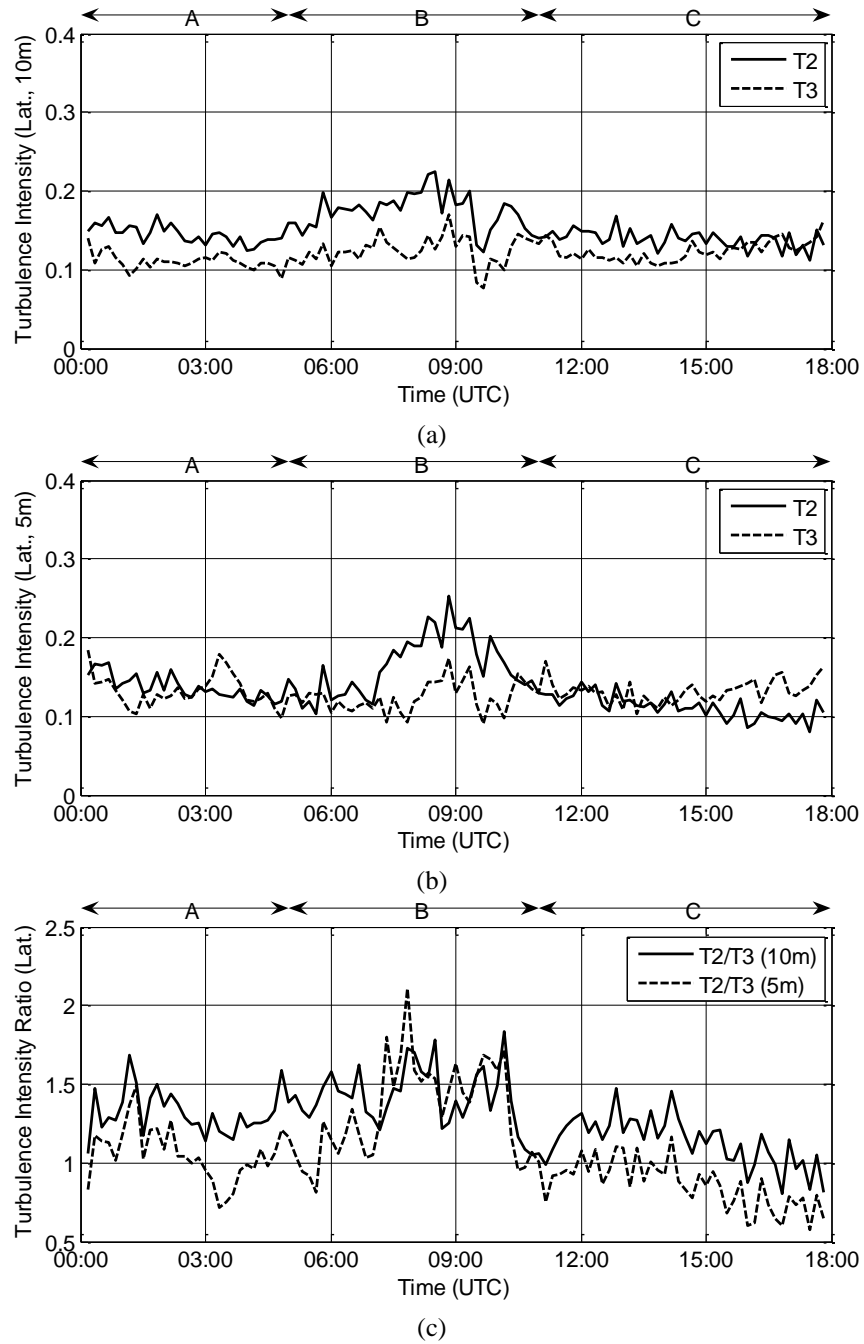


Fig. 9 Time history of (a) lateral turbulence intensities (10 m), (b) lateral turbulence intensities (5 m) and (c) their ratio between T2 and T3

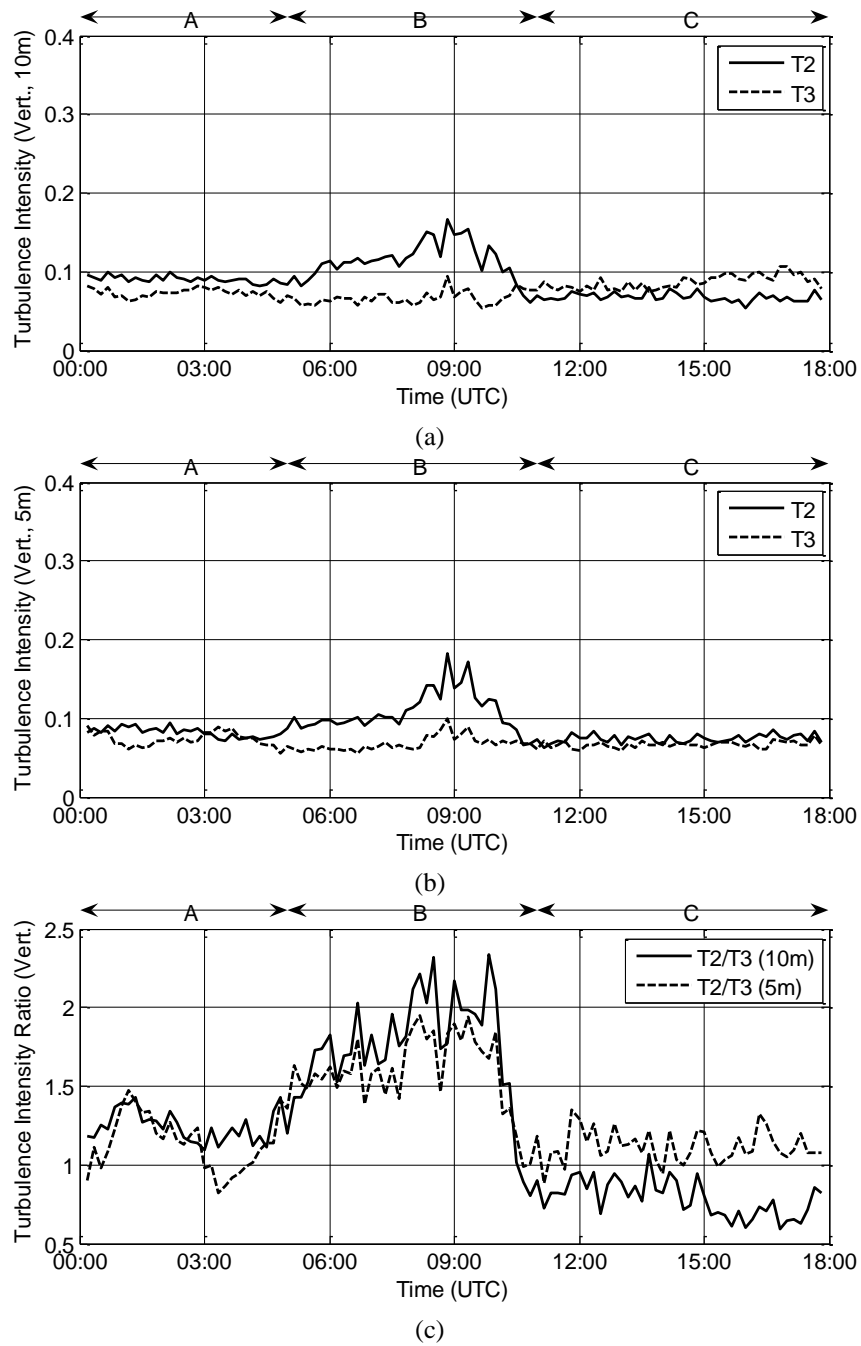


Fig. 10 Time history of (a) vertical turbulence intensities (10 m), (b) vertical turbulence intensities (5 m), and (c) their ratio between T2 and T3

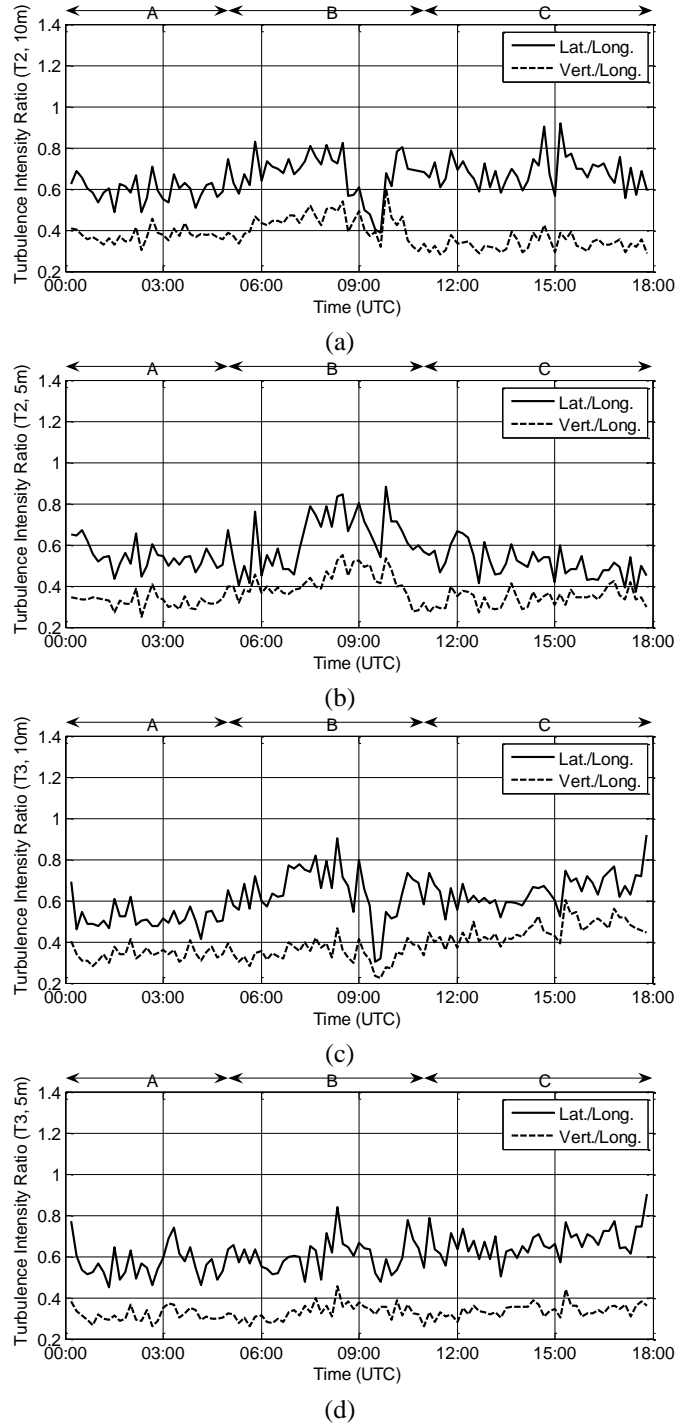


Fig. 11 The ratio between the lateral and the longitudinal turbulence intensities, and the vertical and the longitudinal turbulence intensities ((a) T2, 10 m, (b) T2, 5 m, (c) T3, 10 m and (d) T3, 5 m)

8. Comparison of integral length scales

Integral scales of turbulence quantify the average size of the turbulent eddies of the wind. Among nine possible integral scales due to three dimensions of the eddies and the three components of fluctuating velocity, the longitudinal integral scale L_u^x is commonly studied to characterize the turbulence of the wind. L_u^x is a measure of the average longitudinal size of the eddies associated with the longitudinal velocity fluctuation.

$$L_u^x = \bar{U} \int_0^{\infty} \rho_{uu}(\tau) d\tau \quad (6)$$

$$\rho_{uu}(\tau) = \frac{E[u(t)u(t+\tau)]}{\sigma_u^2} \quad (7)$$

in which \bar{U} is the mean speed for a predefined time period, ρ_{uu} is the autocorrelation function, u is the fluctuating component, σ_u is the standard deviation of the wind, and $E[\cdot]$ is the expected value operator. Due to the non-stationarity of the data, \bar{U}' is used for the mean speed and Eq. (4) with the root mean square is used to calculate the standard deviation (Chen *et al.* 2007).

Large magnitudes of L_u^x indicate that stronger correlation exists between the fluctuating components $u(t)$ and $u(t+\Delta\tau)$ over the time scale, L_u^x / U . It is known that L_u^x increases if terrain surface becomes smoother (Counihan 1975). Another factor that affects the magnitude of L_u^x is the length of the segment. In theory, infinite length of segment is used in the definition, but in practice, finite length of segment is used. In this paper, 10-min segments are used to be consistent with all other quantities that also used 10-min segments. Segments in which the average speed is less than 10 m/s are not included in the analysis. Most of these segments are during the eyewall passage with high non-stationarity. Even after the de-trending process, some of them produced unreliable result for the autocorrelation. Two segments between UTC 9:40~10:00 are also excluded in which integral scales for T3 were unrealistically high. Out of 107 segments, 93 segments are used for T2 and 96 segments are used for T3.

Fig. 12 shows the autocorrelation coefficients in UTC 1:40~1:50 and UTC 10:20~10:30. When both towers have similar magnitude of the turbulence intensity in UTC 1:40~1:50, the autocorrelation coefficients are similar because the average size of the turbulent eddies would be similar. When the turbulence intensity of T2 is much greater than that of T3 in UTC 10:20~10:30, the autocorrelation coefficients of T2 becomes much smaller than those of T3. The increased turbulence generally reduces the correlation of the fluctuating component $u(t)$ and $u(t+\Delta\tau)$.

Fig. 13 shows time history of the longitudinal integral scales of T2 and T3. The figure clearly shows the increase of the integral scales of T3 in Interval B, where T3 has open terrain. The mean value of the integral scales of T3 in Interval B is 197 m, which is comparable to "open land" integral scales of the Hurricane Ivan (240 m, 366 m) and the Hurricane Lili (226 m) reported in Yu *et al.* (2008). As reported in Chen *et al.* (2007), the integral length scale obtained by the non-stationary model of this paper is smaller than that obtained by the traditional model used in Yu *et al.* (2008). The mean value of the integral scales of T2 in Interval B is 166 m (131 m when an outlier in UTC 5:10~5:20 is excluded). Except 2~3 outliers in each Interval, Intervals A and C

show similar magnitude of the integral scales for T2 and T3. Further details of the statistics of the integral scales are summarized in Table 7. The values are comparable to previously reported values summarized in Counihan (1975).

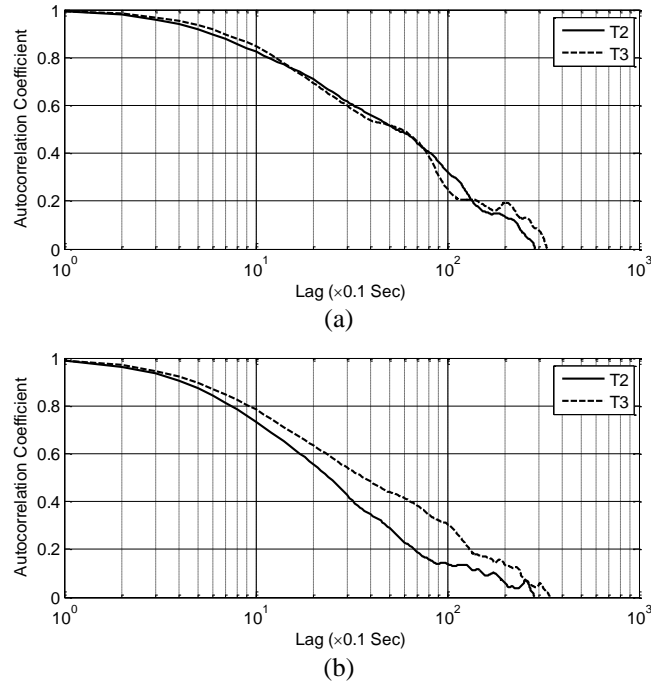


Fig. 12 Autocorrelation coefficients when (a) the turbulence intensity of both towers are similar (Interval A, UTC 1:40~1:50) and (b) the turbulence intensity of T2 is much greater than T3 (Interval B, UTC 10:20~10:30)

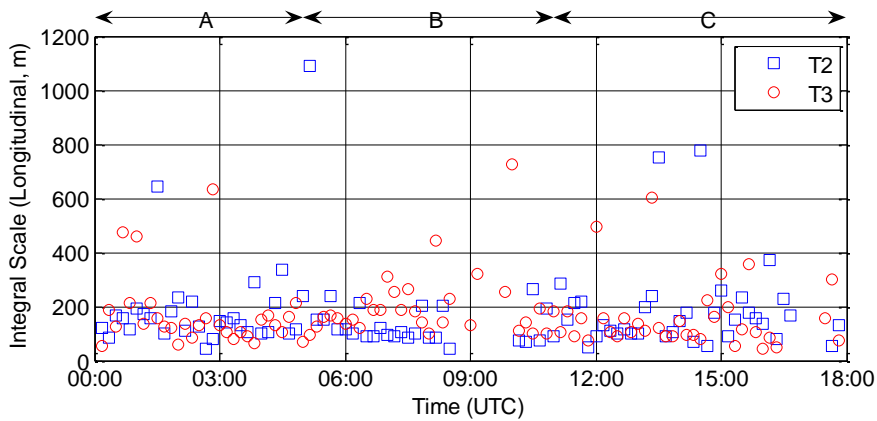


Fig. 13 Time history of the longitudinal integral scales of T2 and T3

Table 7 Statistics of the longitudinal integral scales of T2 and T3 (*: when an outlier in UTC 5:10~5:20 is excluded)

Interval ID	Statistical measure	T2	T3
A	Mean	167.0	171.2
	Standard deviation	111.1	131.1
B	Mean	166.1 (130.5*)	197.3
	Standard deviation	194.7 (62.1*)	126.3
C	Mean	183.0	158.2
	Standard deviation	157.7	120.4

9. Comparison of power spectra

The longitudinal power spectral density function describes the frequency distribution of turbulent along-wind velocity component u (Dyrbye and Hansen 1997). It is typically normalized as

$$R_N(z, n) = \frac{nS_{uu}(z, n)}{\sigma_u^2(z)} \quad (8)$$

in which n is the frequency in hertz, $S_{uu}(z, n)$ is the power spectral density (PSD) for the along-wind turbulence component, and σ_u is the standard deviation of the wind. Lateral and vertical spectra can be similarly computed.

In order to compare the power spectra of T2 and T3, Fast Fourier Transform (FFT) using the Welch method (Welch 1967) is employed. From each Interval, the 4-hour time series are segmented into 10-minute sub-segments with a 50% overlap and tapered with a Hamming window. The final PSD is based on the average of these individual segments. Once the PSD is obtained, it is normalized following the Eq. (8). The spectra are plotted against the reduced frequency nz/\bar{U} in Fig. 14.

Due to the mechanical characteristics of the anemometers, the spectra at reduced frequency at or below 0.1 are more accurate than the spectra at higher reduced frequencies (Schroeder and Smith 2003). For the spectra at higher frequencies, other non-hurricane based spectra may be used with satisfactory accuracy (Yu *et al.* 2008). The symbols “□” and “○” in Fig. 14 show the obtained longitudinal power spectra. As expected, power spectra between T2 and T3 do not show much difference in Intervals A and C. In Interval B, T3 contains more low-frequency energy than T2. The higher values of spectra for open terrain (T3) is consistent with the previous study (Yu *et al.* 2008) in which sea surface had higher values of spectra compared to open land. Interestingly, T2 shows more high-frequency energy beyond the reduced frequency of 0.1. However, the values at this region are not as reliable as the low-frequency region due to the reasons noted earlier.

The spectra from T2 and T3 are further compared with models by other researchers. The general expression for the spectra at certain height is (Geurts 1997)

$$\frac{nS_{uu}}{\sigma_u^2} = \frac{Af^\gamma}{(C + Bf^\alpha)^\beta} \quad (9)$$

in which factors $\alpha, \beta, \gamma, A, B,$ and C for the models compared in this paper are shown in Table 8. “Tieleman FSU terrain” is for flat, smooth, and uniform terrain, whereas “Tieleman perturbed” is for terrain with some obstacles (Tieleman 1995). “Kaimal” is developed using the data from flat, uniform terrain in Kansas (Kaimal *et al.* 1972). All models are based on non-hurricane winds.

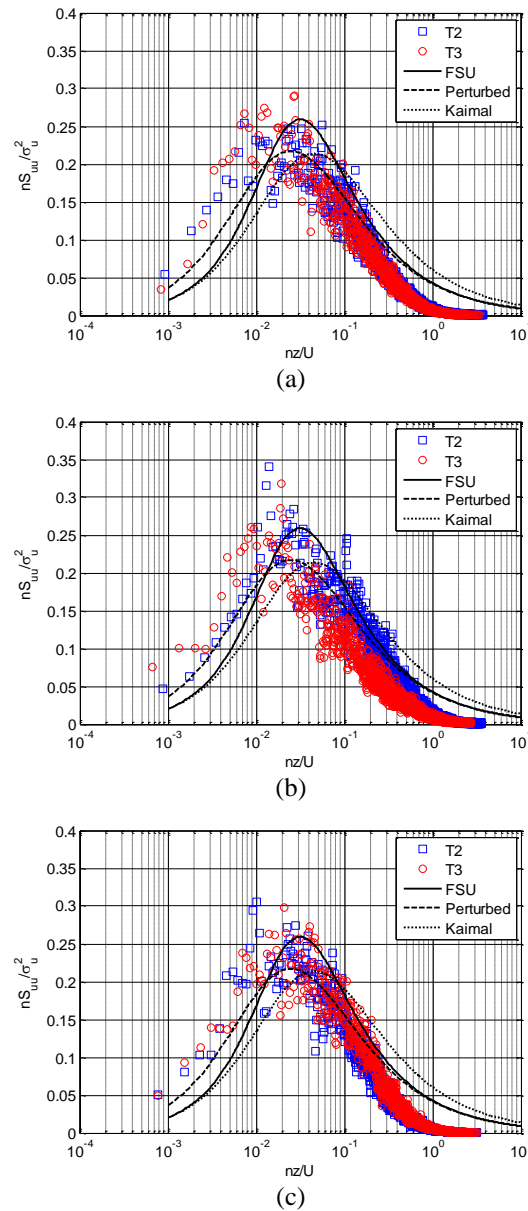


Fig. 14 Longitudinal wind spectra (10 m) of (a) Interval A (UTC 1:00~5:00), (b) Interval B (UTC 6:00~10:00) and (c) Interval C (UTC 12:00~16:00)

Table 8 Factors for the general spectra model (adapted from (Geurts 1997))

	Tieleman FSU terrain		Tieleman perturbed terrain		Kaimal	
	$C = 1, \alpha = 5/3, \beta = 1, \gamma = 1$		$C = 1, \alpha = 1, \beta = 5/3, \gamma = 1$		$C = 1, \alpha = 1, \beta = 5/3, \gamma = 1$	
S_{uu}	A	B	A	B	A	B
	20.53	475.1	40.42	60.62	21.66	33

Spectra from these models are shown in Fig. 14 as solid, dashed, and dotted lines. In all cases, more low-frequency energy of T2 and T3 is distinctively shown, which is consistent with previous studies by other researchers (Schroeder and Smith 2003, Yu *et al.* 2008). The mid-frequency range does not show much difference between the tower-spectra and other models. As noted earlier, high-frequency range of tower-spectra is not reliable and other models would provide more accurate estimation (also see discussions in (Yu *et al.* 2008)). Compared to the spectra models shown as lines, the discrete points obtained from the measured data show irregularity. If one needs to obtain spectral curves using the discrete points, incorporation of physical behavior will improve the quality of the obtained curves (Caracoglia and Jones 2009, Li *et al.* 2012), rather than using all data points in curve fitting.

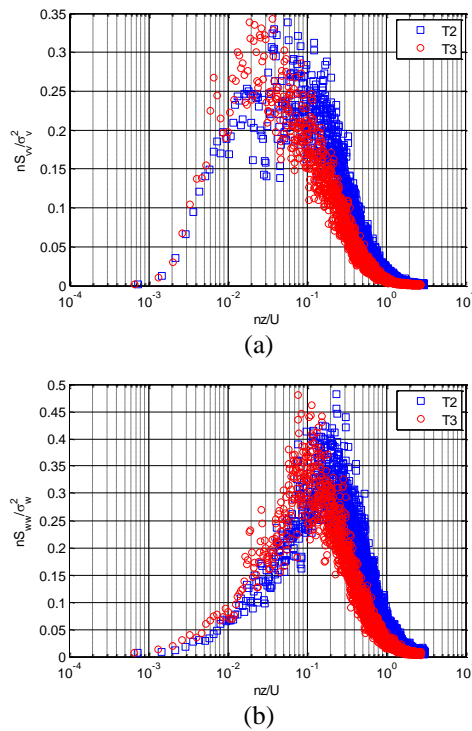


Fig. 15 (a) Lateral and (b) vertical wind spectra (10 m) of Interval B (UTC 6:00~10:00)

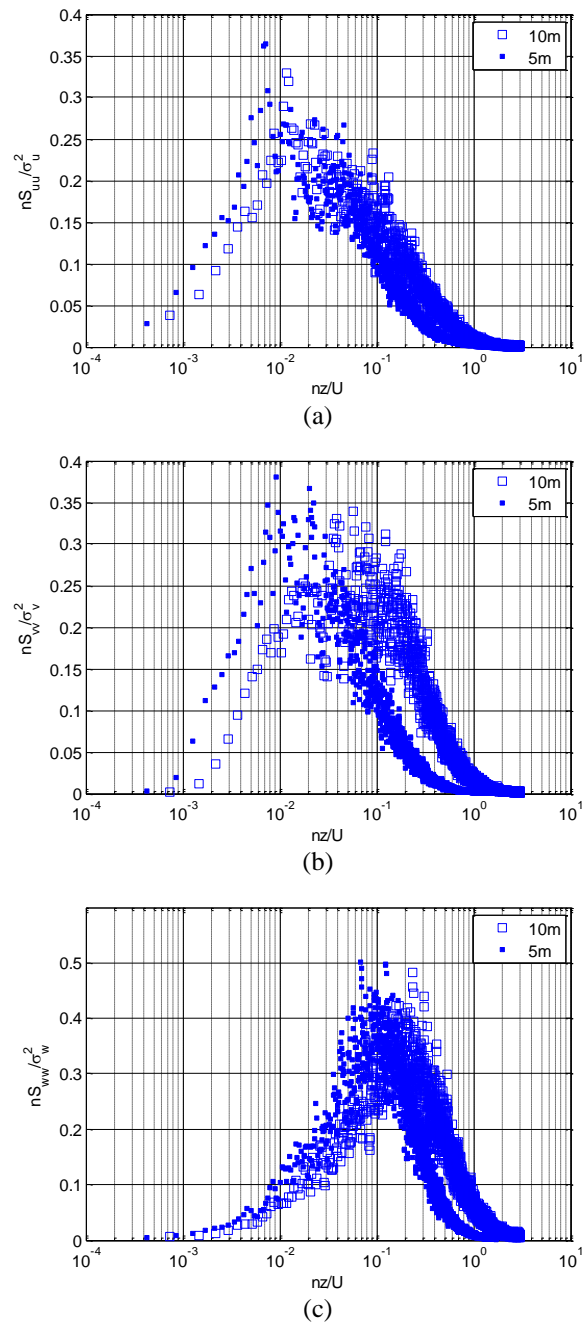


Fig. 16 Comparison of 10m and 5m spectra (all from T2: (a) longitudinal, (b) lateral and (c) vertical)

For the Interval B, additional spectra are plotted for further analysis. Fig. 15 shows lateral and vertical spectra at 10 m, which show similar trend as the longitudinal spectra of Fig. 14(b). Fig. 16 compares 10 m spectra and 5 m spectra. Overall, 5 m spectra show higher values below the reduced frequency of 0.1, especially for the vertical spectra. This observation is consistent with the previous findings by Yu *et al.* (2008). Another interesting comparison is shown in Fig. 17. Unlike 10 m spectra in which T3 was notably higher than T2 below the reduced frequency of 0.1, the 5m spectra do not show much difference between T2 and T3 except the vertical spectra. Even for the vertical spectra, the difference is not as significant as that of 10 m spectra.

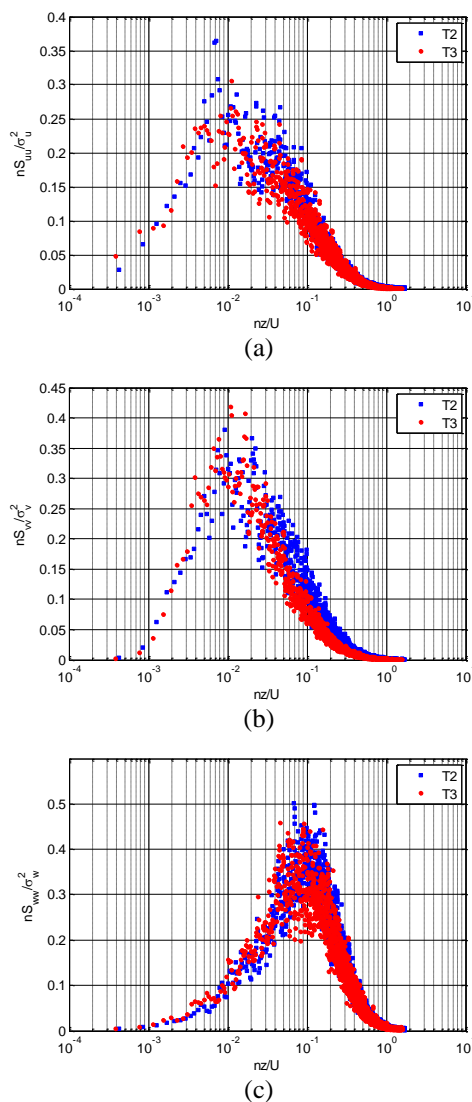


Fig. 17 (a) Longitudinal, (b) lateral and (c) vertical wind spectra (5 m) of Interval B (UTC 6:00~10:00)

10. Conclusions

During Hurricane Ike, two mobile instrumented towers were co-located 2.2 km apart but in differing terrain conditions. During the most intense interval of the storm, the upwind terrain characteristics were primarily suburban and open. The data collected and analyzed in this paper is the first attempt to compare the terrain effect of two nearby regions simultaneously during a hurricane. The conclusions of the research are:

(1) The mean gust factors of open terrain is 1.49, which is comparable to the previous study by Vickery and Skerlj (2005) who reported the 10-min mean gust factor of 1.55. The mean gust factor of suburban terrain is 1.73.

(2) Many 1-hour segments of wind data, especially when the wind direction abruptly changed, showed significant level of non-stationarity. Empirical mode decomposition was effective in de-trending the signal for further analysis of turbulence. Without the de-trending, the turbulence intensity is overestimated.

(3) Although the empirical mode decomposition was effective in addressing the first order non-stationarity, it did not resolve any non-stationarity of the variance. To resolve this issue, more theoretical work needs to be conducted, which is left for the future research. In this paper, all analyses used 10-min segments to minimize the effect of the non-stationarity of the standard deviation.

(4) The mean longitudinal turbulence intensity of the suburban terrain at a 10 m height is 0.265 and that of the open terrain is 0.196. At a 5 m height, the difference is smaller. For the suburban terrain, the turbulence intensity shows clearly decreasing trend when the mean wind speed increases. For the open terrain, the turbulence intensity does not change much due to the change in the mean wind speed.

(5) The longitudinal integral length scale of the suburban terrain is 166 m (131 m when an outlier in UTC 5:10~5:20 is excluded) whereas that of the open terrain is 197 m. The integral scale of the open terrain is comparable to "open land" integral scales of the Hurricane Ivan (240 m, 366 m) and the Hurricane Lili (226 m) reported in Yu *et al.* (2008).

(6) In the analysis of along-wind 10 m spectra, the energy in low frequencies is significantly higher than non-hurricane spectral models (Tieleman 1995, Kaimal *et al.* 1972), which is consistent with previous studies by other researchers (Schroeder and Smith 2003, Yu *et al.* 2008). The open terrain shows more low frequency energy than the suburban terrain. The 5 m spectra show higher values than the 10 m spectra below the reduced frequency of 0.5. The terrain difference is not as distinctive in 5 m spectra as in 10 m spectra.

Acknowledgements

The authors wish to thank the State of Florida Department of Community Affairs, the National Oceanic and Atmospheric Administration and the Federal Emergency Management Agency for supporting deployment activities in Atlantic tropical cyclones. Special appreciation is extended to Risk Management Solutions, Inc., the Institute for Business and Home Safety, the Federal Alliance for Safe Homes and Mr. William Riker, President of Riker Consulting. This work was also supported in part by the National Science Foundation under grant number CMMI-1055744. Any opinions, findings, and conclusions or recommendations expressed in this material are those of the authors and do not necessarily reflect the views of the sponsors.

References

- Andreas, E.L., Geiger, C.A., Trevino, G. and Claffey, K.J. (2008), "Identifying nonstationarity in turbulence series", *Bound. - Lay. Meteorol.*, **127**(1), 37-56.
- ASCE 7-10 (2010), *Minimum design loads for buildings and other structures*, American Society of Civil Engineers, Reston, VA.
- Baas, P., Bosveld, F.C., Klein Baltink, H. and Holtslag, A.A.M. (2009), "A climatology of nocturnal low-level jets at Cabauw", *J. Appl. Meteorol. Clim.*, **48**(8), 1627-1642.
- Balderrama, J.A., Masters, F.J., Gurley, K.R., Prevatt, D.O., Aponte-Bermúdez, L.D., Reinhold, T.A., Pinelli, J.P., Subramanian, C.S., Schiff, S.D. and Chowdhury, A.G. (2011), "The Florida Coastal Monitoring Program (FCMP): a review", *J. Wind Eng. Ind. Aerod.*, **99**(9), 979-995.
- Bendat, J.S. and Piersol, A.G. (1986), *Random data: analysis and measurement procedures*, Wiley, New York.
- Brown, D.P., Beven, J.L., Franklin, J.L. and Blake, E.S. (2010), "Atlantic hurricane season of 2008", *Mon. Weather. Rev.*, **138**(5), 1975-2001.
- Caracoglia, L. and Jones, N.P. (2009), "Analysis of full-scale wind and pressure measurements on a low-rise building", *J. Wind Eng. Ind. Aerod.*, **97**(5-6), 157-173.
- Chen, J. and Xu, Y.L. (2004), "On modelling of typhoon-induced non-stationary wind speed for tall buildings", *Struct. Des. Tall Spec.*, **13**(2), 145-163.
- Chen, J., Hui, M.C.H. and Xu, Y.L. (2007), "A comparative study of stationary and non-stationary wind models using field measurements", *Bound.- Lay. Meteorol.*, **122**(1), 105-21.
- Counihan, J. (1975), "Adiabatic atmospheric boundary layers: a review and analysis of data from the period 1880-1972", *Atmos. Environ.*, **9**(10), 871-905.
- Dyrbye, C. and Hansen, S.O. (1997), *Wind loads on structures*, Wiley, New York.
- ESDU (1983), "Strong winds in the atmospheric boundary layer, part 2: discrete gust speeds", Item No. 83045.
- Geurts, C.P.W. (1997), *Wind-induced pressure fluctuations on building facades*, doctoral thesis, Technische Universiteit Eindhoven.
- Harris, R.I. and Deaves, D.M. (1981), *The structure of strong winds*,
- Huang, N.E. (2005), *Hilbert-huang transform and its applications*, World Scientific, New Jersey.
- Huang, N.E., Shen, Z., Long, S.R., Wu, M.C., Shih, H.H., Zheng, Q., Yen, N., Tung, C.C. and Liu, H.H. (1998), "The empirical mode decomposition and the Hilbert spectrum for nonlinear and non-stationary time series analysis", *Proceedings of the Mathematical, Physical and Engineering Sciences*, **454**(1971), 903-995.
- Ishizaki, H. (1983), "Wind profiles, turbulence intensities and gust factors for design in typhoon-prone regions", *J. Wind Eng. Ind. Aerod.*, **13**(1-3), 55-66.
- Izumi, Y. (1971), "Kansas 1968 field program data report", AFCRL-TR-72-0041.
- Izumi, Y. and Caughey, J.S. (1976), "Minnesota 1973 atmospheric boundary layer experiment data report", AFCRL-TR-76-0038.
- Kaimal, J.C., Wyngaard, J.C., Izumi, Y. and Coté, O.R. (1972), "Spectral characteristics of surface-layer turbulence", *Q. J. Roy. Meteorol. Soc.*, **98**(417), 563-589.
- Krayer, W.R. and Marshall, R.D. (1992), "Gust factors applied to hurricane winds", *B. Am. Meteorol. Soc.*, **73**(5), 613-618.
- Lettau, H.H. and Davidson, B. (1957), *Exploring the atmosphere's first mile*, Pergamon Press, New York, NY.
- Li, Q.S., Zhi, L. and Hu, F. (2009), "Field monitoring of boundary layer wind characteristics in urban area", *Wind Struct.*, **12**(6), 553-574.

- Li, L., Xiao, Y., Kareem, A., Song, L. and Qin, P. (2012), "Modeling typhoon wind power spectra near sea surface based on measurements in the South China sea", *J. Wind Eng. Ind. Aerod.*, **104-106**, 565-576.
- Lilliefors, H.W. (1967), "On the Kolmogorov-Smirnov test for normality with mean and variance unknown", *J. Am. Stat. Assoc.*, **62**(318), 399-402.
- Masters, F.J., Vickery, P.J., Bacon, P. and Rappaport, E.N. (2010). "Toward objective, standardized intensity estimates from surface wind speed observations", *B. Am. Meteorol. Soc.*, **91**, 1665-1682.
- Masters, F.J., Tieleman, H.W. and Balderrama, J.A. (2010), "Surface wind measurements in three Gulf Coast hurricanes of 2005", *J. Wind Eng. Ind. Aerod.*, **98**(10-11), 533-547.
- Schroeder, J.L. and Smith, D.A. (2003), "Hurricane Bonnie wind flow characteristics as determined from WEMITE", *J. Wind Eng. Ind. Aerod.*, **91**(6), 767-789.
- Taylor, P.A. and Teunissen, H.W. (1987), "The Askervein Hill project: overview and background data", *Bound.- Lay. Meteorol.*, **39**(1-2), 15-39.
- Tieleman, H.W. (1995), "Universality of velocity spectra", *J. Wind Eng. Ind. Aerod.*, **56**(1), 55-69.
- Vickery, P.J. and Skerlj, P.F. (2005), "Hurricane gust factors revisited", *J. Struct. Eng.*, **131**(5), 825-832.
- Welch, P. (1967), "The use of fast Fourier transform for the estimation of power spectra: a method based on time averaging over short, modified periodograms", *IEEE T. Audio Electr.*, **5**(2), 70-73.
- Wieringa, J. (1973), "Gust factors over open water and built-up country", *Bound.- Lay. Meteorol.*, **3**(4), 424-441.
- Xu, Y.L. and Chen, J. (2004), "Characterizing nonstationary wind speed using empirical mode decomposition", *J. Struct. Eng.*, **130**(6), 912-920.
- Yu, B., Chowdhury, A.G. and Masters, F. (2008), "Hurricane wind power spectra, cospectra, and integral length scales", *Bound.- Lay. Meteorol.*, **129**(3), 411-30.